Supplement

Supplemental Figure Legends

Fig. S1. (**a**) Generation of bigenic offspring from heterozygous Six2-GFPCre^{+} mice and homozygous iDTR^{+} mice. Inheritance of transgenes occurred at mendelian ratios. Animals testing positive for both transgenes (Six2-GFPCre^{+};iDTR^{+}) were considered bigenic and labeled DTR^{rec} (here animals 2, 3, 4). Single transgenic littermates (here animals 1, 5) and vehicle (PBS)-treated DTR^{rec} mice served as controls. (**b**) In adult DTR^{rec} mice, renal epithelial cells rendered susceptible to DT (blue) are expected to include proximal and distal tubules, but not collecting ducts due to their ureteric bud lineage. (**c**) Comparison of body weight between bigenic DTR^{rec} and littermate control mice. Data are given as mean ± SEM. (**d**) Comparison of glomerular counts between bigenic DTR^{rec} and littermate controls, indicating no significant difference in glomerular endowment. Data points represent counts/section of individual animals, horizontal lines represent mean values.

Fig. S2. Vessels are not affected by DT in kidneys of DTR^{rec} mice. (**a**&**b**) H&E stained micrographs of DTR^{rec} kidneys three days after administration of a single lethal dose of DT. Note regular morphology of vessels *(asterisk)*. By contrast, surrounding tubules exhibit signs of severe injury. Scale bars: 50µm. (**c**) EM micrograph showing normal vessel ultrastructure in a DTR^{rec} kidney three days after DT treatment. Scale bar: 5µm.

Fig. S3. Distribution of TUNEL+ apoptotic cells in kidneys of DTR^{rec} mice three days after administration of a sublethal (0.15µg/kg) or lethal (0.25µg/kg) dose of DT. (**a**&**b**) Costaining with FITC-labeled Lotus tetragonolobus (LTA) lectin (1:500, Vector Labs), which has a high affinity

Formatted: Justified
Formatted: Font: Bold
Formatted: Superscript
Formatted: Font: Bold
Formatted: Font: Bold
Formatted: Superscript
Formatted: Font: Italic
Formatted: Font: Bold
Formatted: Superscript
Formatted: Font: Bold
Formatted: Justified
Formatted: Superscript
Formatted: Font: Bold
Formatted: English (U.S.)

for the apical aspect of proximal tubules, shows that the vast majority of apoptotic cells (TUNEL$^+$ nuclei) in sublethally injured DTR^{rec} kidneys are located in LTA$^+$ proximal tubules and in close association with glomeruli thus consistent with S1/S2 segments. By contrast, no apoptotic bodies were observed in glomerular tufts (G) or in FITC-labeled Dolichos biflorus agglutinin (DBA) lectin$^+$ (1:500, Vector Labs) collecting ducts (basolateral staining). Note loss of LTA affinity in lethally injured kidneys due to increased severity of damage in proximal tubules. Scale bars: 50µm, n=4-5 per group.

Fig. S42. (**a**) Electronmicrograph shows, at higher power, degenerated epithelial cells at the glomerulotubular junction with nuclear condensation *(asterisk)*, segmental loss of brush border and cytoplasmic debris within the urinary space. Note intact podocytes with complete preservation of foot processes in immediate proximity. Scale bar: 2µm. (**b**) Staining with Kim-1-specific antibody. *Left:* Representative micrographs show substantial induction of Kim-1 in apical aspects of selected tubules in DTR^{rec} kidney cortex 3 days after DT administration. Scale bar: 50µm. *Right*: ~~Semi-automated~~ Quantitative time course analysis of Kim-1$^+$ fluorescence area demonstrates the appearance of Kim-1 as early as ~~24~~ 1 day ~~hours~~ and ~~culminating~~ increasing at 3 days after DT injection. Values are shown as mean ± SEM, n=3-4 for each data point; **P*<0.01. (**c**) Electropherograms of urine samples from the same DTR^{rec} mouse obtained at baseline ~~(0d)~~ and at various time points after DT administration. Note transient appearance of additional peaks (*arrow head*) in the size range of 60 to 75 kDa ~~and thus~~ consistent with albumin at 3 days after injection. (**d**) Fragmentation and quantitative analysis of urinary protein fractions reveals a relative increase of proteins >50 kDa, peaking at day 3 after DT injection and returning to baseline levels thereafter. Values are given as mean ± SEM, n=3-6 for each data point; **P*<0.01, ***P*<0.001 vs. baseline (0d). (**e**) Reagent strip-based estimate of urinary albumin in DTR^{rec} and littermate control mice before and at various time points after DT administration.

Formatted: English (U.S.)
Formatted: Superscript
Formatted: Superscript
Formatted: Superscript
Formatted: Font: (Default) Arial
Formatted: Font: (Default) Arial, Superscript
Formatted: Font: (Default) Arial
Formatted: English (U.S.)
Formatted: Superscript

In support of the chip data, the findings indicate a significant but reversible increase in urinary albumin after DT-induced injury showing normalization by day 14 after injection (1=trace, 2=30mg/dL, 3=100mg/dL, 4=300mg/dL, 5=2000mg/dL or more). Data points represent measurements of individual animals, horizontal lines represent mean values; *P<0.0001, **P<0.00001.

Fig. S5. Distribution of Ki67$^+$ proliferating epithelial cells in kidneys of DTR^{rec} mice at day 3 after administration of a sublethal (0.15µg/kg) or lethal (0.25µg/kg) dose of DT. (**a**-**c**) Double-staining of kidney sections with anti-Ki67 antibody/FITC-labeled LTA and anti-Ki67 antibody/FITC-labeled DBA shows that the majority of Ki67$^+$ epithelial cells are located in LTA$^+$ proximal tubules in sublethally injured DTR^{rec} kidneys. The prevalence of Ki67$^+$ cells in glomerular tufts or DBA$^+$ collecting ducts is low and comparable between sublethally and lethally injured DTR^{rec} kidneys. Note again loss of LTA affinity in lethally injured kidneys due to widespread and severe damage of the proximal tubular epithelium. Scale bars: 50µm.

Fig. S64. (**a**) Quantitative analysis of proliferative activity by Ki67-specific staining of kidney sections from repeatedly (3x at weekly intervals) DT-treated (0.15µg/kg) DTR^{rec} and control mice at 5 weeks after the first treatment. *Left:* Representative micrographs of renal cross sections stained with anti-Ki67 antibody. Scale bar: 20µm. *Right:* Quantitation demonstrates strong increases in Ki67+ cells in the tubular ~~o~~epithelium as well as the interstitium of ~~repeatedly~~ DT-injured kidneys. Values are given as mean ± SEM, n=3 for each data point; *P<0.001. (**b** & **c**) Additional cell type-specific immunostaining and quantification of chronically injured DTR^{rec} and uninjured littermate control kidneys. *Left:* Representative micrographs of sections stained for αSMA (myofibroblasts) and FSP-1/S100A4. Scale bars: 20µm. *Right:* Comparative

Formatted: Font: Bold
Formatted: Superscript
Formatted: Font: Not Bold
Formatted: Font: Bold
Formatted: Superscript
Formatted: Superscript
Formatted: Superscript
Formatted: Superscript
Formatted: Superscript
Formatted: Superscript

quantifications of fluorescence area per high power field and cell counts, respectively, reveal an increase in myofibroblasts and FSP-1^{+} cells in the expanded tubulointerstitium of repeatedly DT-injured kidneys from DTR^{rec} mice. Values are given as mean ± SEM, n=3-5 for each data point; *P<0.05, **P<0.001.

Supplemental Figure S1

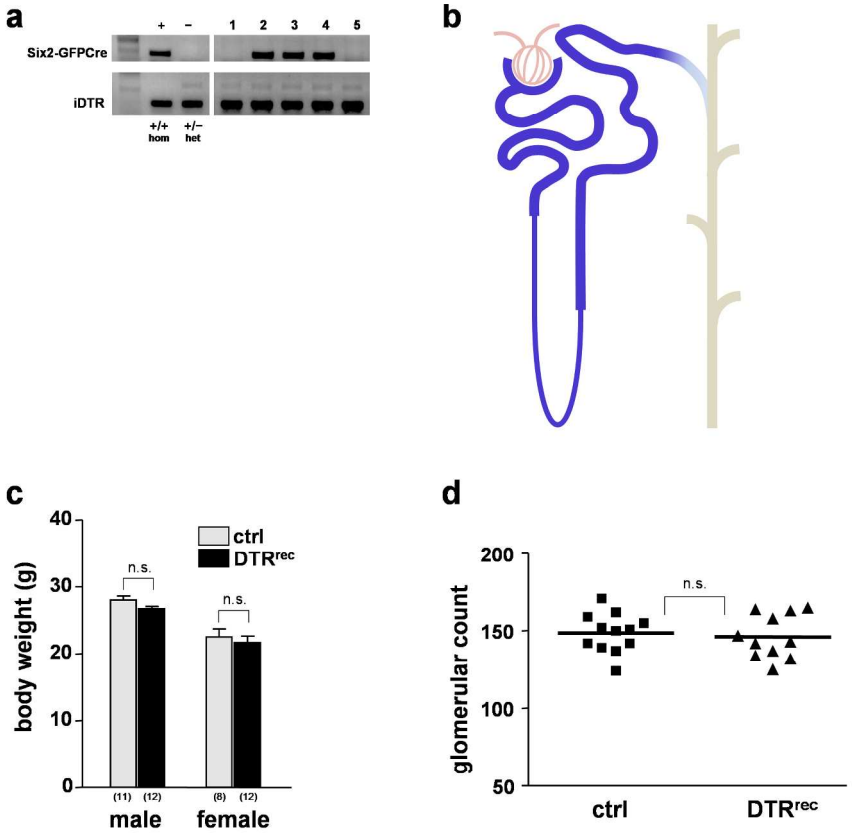

190x254mm (300 x 300 DPI)

Supplemental Figure S2

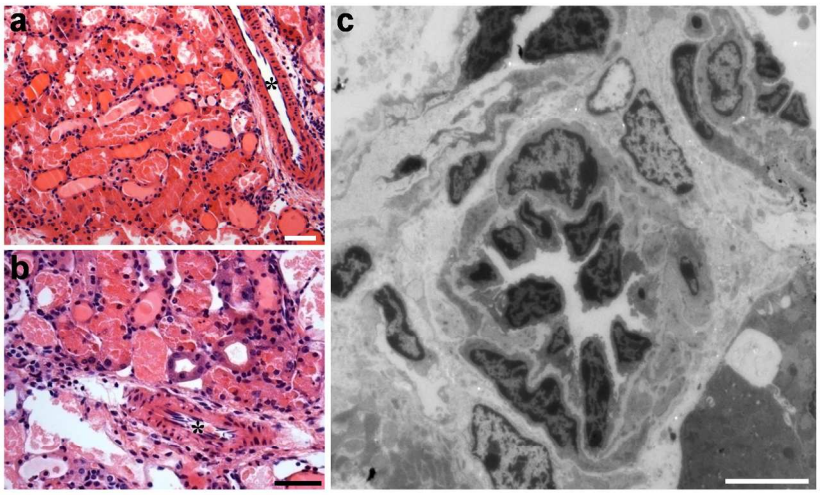

190x254mm (300 x 300 DPI)

Supplemental Figure S3

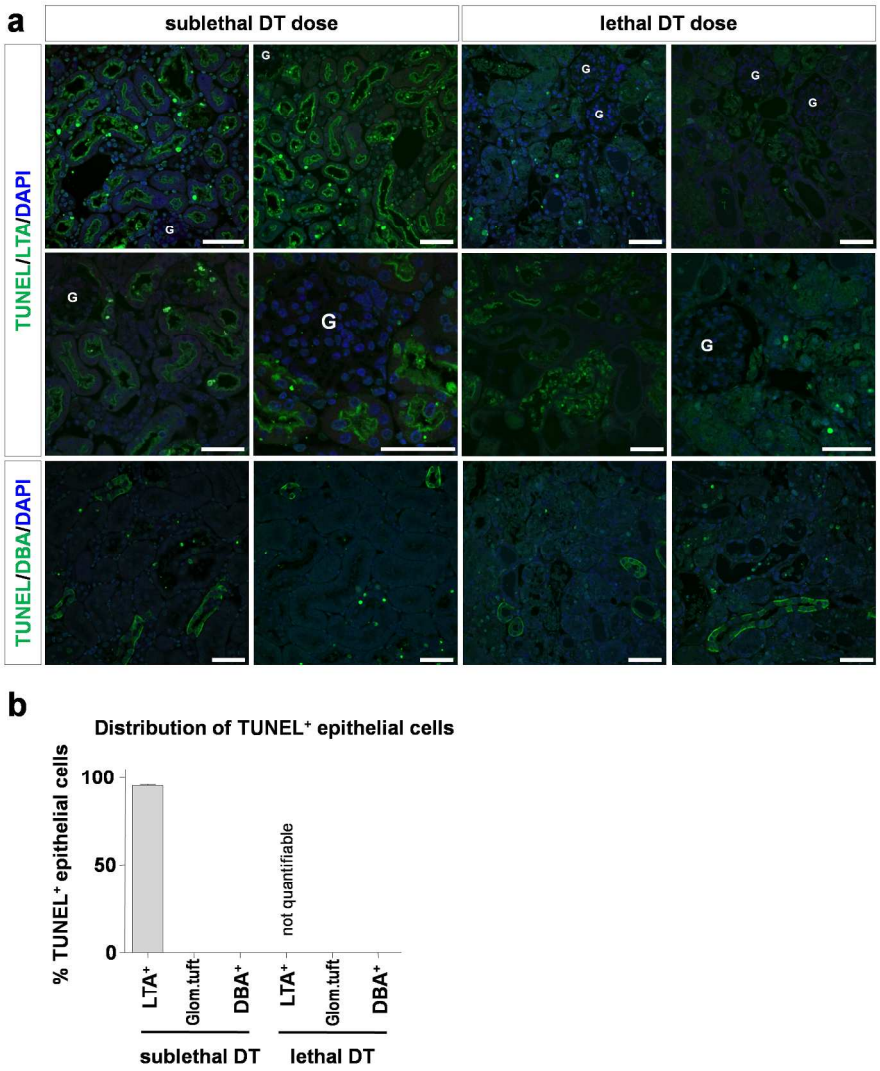

190x254mm (300 x 300 DPI)

Supplemental Figure S4

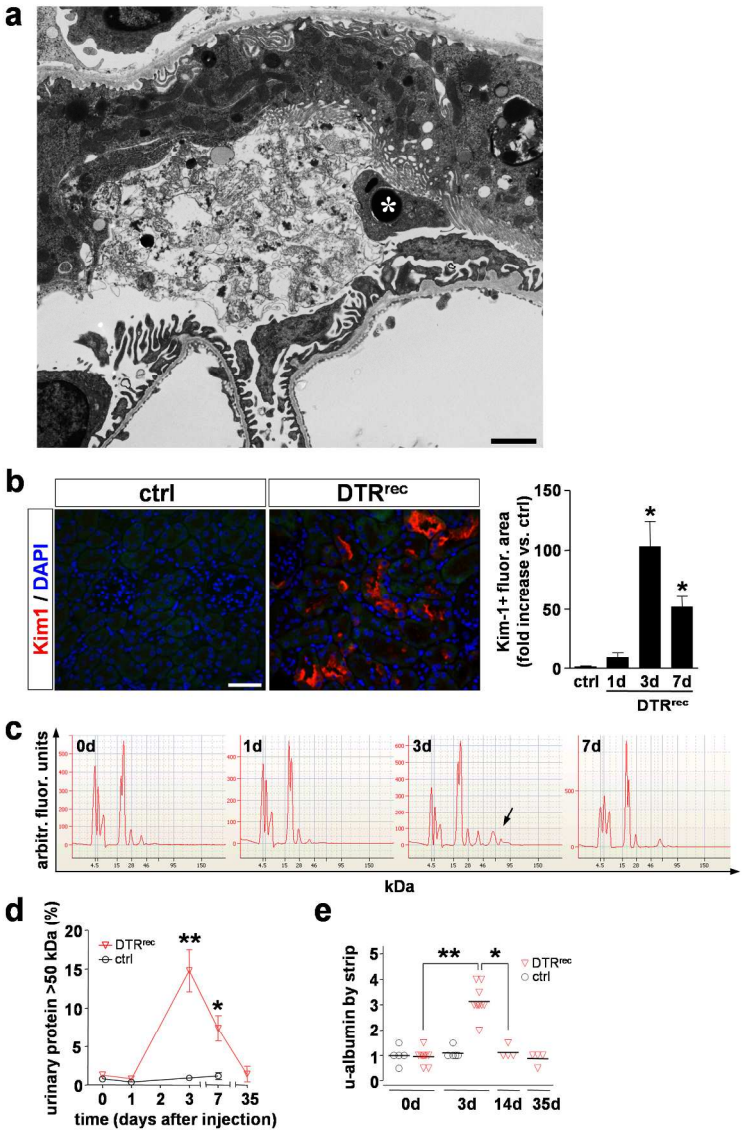

190x254mm (300 x 300 DPI)

Supplemental Figure S5

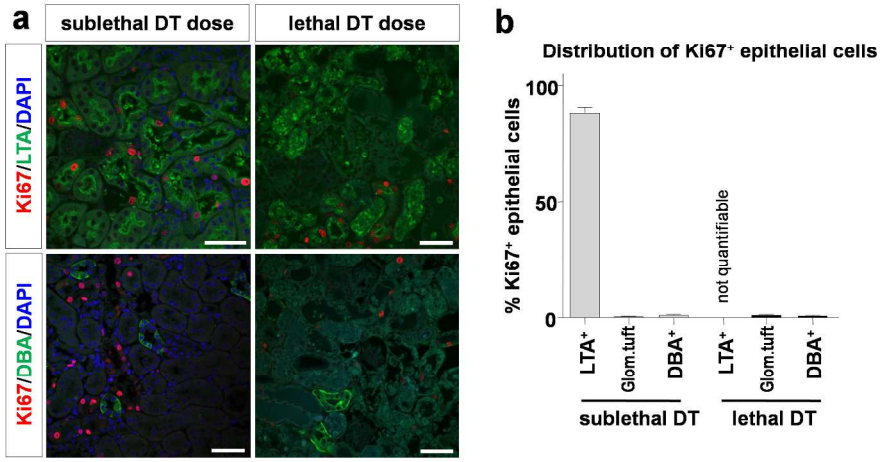

190x254mm (300 x 300 DPI)

Supplemental Figure S6

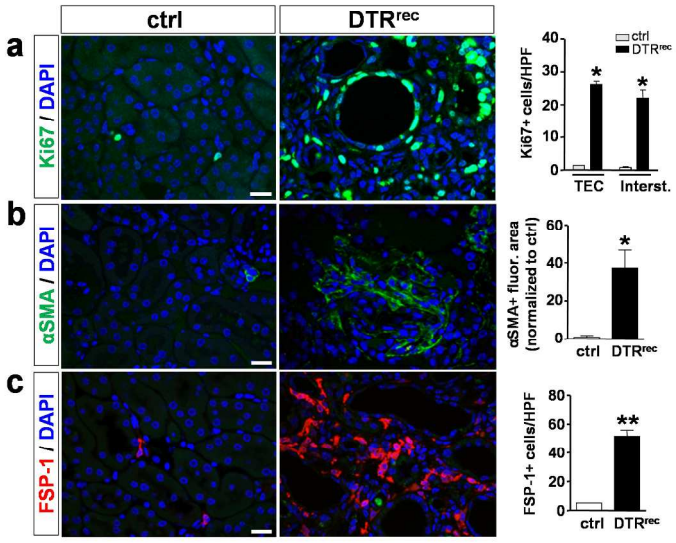

190x254mm (300 x 300 DPI)

Supplement

Materials and Methods

Microbead-based immunoassay

Urine Kim-1 and NGAL protein concentrations were measured using Luminex xMAP technology. Briefly, 30 µl of each protein sample were incubated with ~6000 anti-mouse Kim-1 and anti-mouse NGAL coupled beads/well, respectively, for 1 hr followed by 3 washes with PBST. Samples were then incubated with biotinylated Kim-1 and NGAL detection antibodies for 45 min and washed again 3 times with PBST. Quantification was achieved by incubating samples with picoerythrin-coupled streptavidin (Invitrogen) and excited at 532 nm. The signal from this flourochrome was detected using the Bio-Plex system (BioRad) and is directly proportional to the amount of antigen bound to the microbead surface. Data was interpreted using a 13-point standard five parametric logistic regression model. All samples were analyzed in triplicate and the intra-assay variability was less than 15 %.

Immunofluorescence staining

Immunohistological staining of kidney sections was performed as previously described (Yang et al, Nat. Med., 2010). Briefly, rehydrated paraffin-embedded (3µm) or cryopreserved (7µm) sections were labeled with primary antibodies, including goat anti-Kim-1 (R&D, 1:500), rabbit anti-Tamm-Horsfall/uromodulin (Biomedical Technologies Inc., 1:100), rabbit anti-Ki67 (Vector Labs, 1:200), rat anti-PDGFRβ (ebioscience, 1:200), FITC-conjugated anti-αSMA (Sigma, 1:500), rat anti-CD31 (ebioscience, 1:100), rat anti-F4/80 (Abcam, 1:100), rat anti-BrdU (Abcam, 1:200), rabbit anti-CD3 (Vector Labs, 1:200), rat anti-neutrophil (Santa Cruz, 1:100) and rabbit anti-FSP-1/S100A4 (Abcam, 1:100). Slides were subsequently exposed to corresponding FITC-

or Cy3-conjugated secondary antibodies (Jackson ImmunoResearch) and mounted with DAPI-containing Vectashield mounting medium (Vector Labs). FITC-conjugated Lotus tetragonolobus (LTA) lectin (Vector Labs, 1:500) and FITC-conjugated Dolichos biflorus agglutinin (DBA) lectin (Vector Labs, 1:500) were used to identify proximal tubules and collecting ducts, respectively. Staining was examined by fluorescence microscopy (Nikon C1 confocal and Nikon eclipse 90i) and semi-automated quantitation was performed using ImageJ software (http://rsbweb.nih.gov/ij/).

Formatted: English (U.S.)